Current Research in Pharmacology and Drug Discovery 3 (2022) 100098

Contents lists available at ScienceDirect

Current Research in Pharmacology and Drug Discovery

journal homepage: www.journals.elsevier.com/current-research-in-pharmacology-and-drug-discovery

Pharmacodynamic evaluation of the XOR inhibitor WN1703 in a model of chronic hyperuricemia in rats induced by yeast extract combined with potassium oxonate

Yuanyuan Li [1], Xinying Zhu [1], Fuyao Liu, Wen Peng, Lei Zhang, Jing Li [*]

MOE International Joint Research Laboratory on Synthetic Biology and Medicines, School of Biology and Biological Engineering, South China University of Technology, Guangzhou, 510006, PR China

ARTICLE INFO

Keywords:
Hyperuricemia
Uric acid
XOR inhibitor
Febuxostat
Rat model

ABSTRACT

Hyperuricemia is a common disease caused by a disorder of purine metabolism, which often causes hyperlipidemia and other metabolic diseases. WN1703 was demonstrated to be an effective xanthine oxidoreductase (XOR) inhibitor in our previous study. Here, we evaluated the pharmacodynamic effect of WN1703 on rats suffering from chronic hyperuricemia accompanied by disorders of lipid metabolism. We discovered that WN1703 was an efficacious uric acid (UA)-lowering compound. Simultaneously, it had effect on relieving renal injury, regulating lipid metabolism by reducing levels of triglycerides and low-density lipoprotein-cholesterol, increasing levels of high-density lipoprotein-cholesterol, and improving renal and liver lesions. WN1703 also exhibited anti-inflammatory and antioxidant activity by alleviating the increasing trend of levels of tumor necrosis factor-α, interleukin-1β, monocyte chemoattractant protein-1, and malondialdehyde, and improving the activity of superoxide dismutase and glutathione peroxidase. WN1703 appeared to be more effective than febuxostat in inhibiting XOR and had higher antioxidant activity. In general, the pharmacologic action of WN1703 showed a clear dose–effect relationship.

1. Introduction

Hyperuricemia is caused by a disorder of purine metabolism or reduced excretion of uric acid (UA). Hyperuricemia shows an abnormally high level of UA in blood. With the remarkable improvement in living standards in some parts of the world, intake of sugar, fat, and protein has increased significantly, and the global prevalence of hyperuricemia has shown an increasing trend (Dehlin et al., 2020).

Accumulating evidence suggests that hyperuricemia is an independent risk factor for developing type-2 diabetes mellitus, hypertension, and cardiovascular disease. Hyperuricemia can increase insulin resistance and decrease insulin release. Sensitivity to insulin declines because of the inflammation caused by hyperuricemia (Li et al., 2017a; Lipkowitz, 2012). The abnormality in the UA concentration is closely associated with impaired levels of fasting glucose in men whereas, for women, the association is not obvious (Miyake et al., 2014). One prospective study showed that an increased serum level of UA can induce oxidative stress and increase intima-media thickness, which can lead to hypertension correlated with overt oxidative stress (Gliozzi et al., 2016). One meta-analysis in China discovered that the overall prevalence of atrial fibrillation was much higher in patients with hyperuricemia than that in the general population, and that each 1 mg/dL increase in the serum UA level led to an increase in the risk of atrial fibrillation of 21% (Zhang et al., 2020a). The mechanism of action of hyperuricemia on cardiovascular disease is not known, but emerging evidence suggests that it is related to release of proinflammatory factors caused by hyperuricemia, such as C-reactive protein and interleukin (IL)-6 (Wu et al., 2016).

Abbreviations: ADA, adenosine deaminase; BUN, blood urea nitrogen; CG, control group; CMC-Na, sodium carboxymethyl cellulose; FEB, febuxostat; GSH-PX, glutathione peroxidase; H1703, high dose of WN1703; IL-1β, interleukin-1β; L1703, low dose of WN1703; XOR, xanthine oxidoreductase; M1703, median dose of WN1703; MCP, monocyte chemoattractant protein; MG, model group; TNF-α, tumor necrosis factor-α; UA, uric acid; URAT1, urate transport protein 1; YEP, yeast extract paste.

* Corresponding author.
E-mail address: lij@scut.edu.cn (J. Li).

[1] These authors contributed equally to this work and should be considered as co-first authors.

https://doi.org/10.1016/j.crphar.2022.100098
Received 30 December 2021; Received in revised form 14 March 2022; Accepted 21 March 2022

Inhibitors of xanthine oxidoreductase (XOR; e.g., allopurinol, febuxostat) and urate transport protein 1 (URAT1; e.g., lesinurad, benzbromarone) are the main drug types for treatment of hyperuricemia and gout. Febuxostat (a phenylthiazole derivative with outstanding and longer-lasting XOR inhibitory potency than that of allopurinol) was approved for gout treatment in the USA in 2009. After treatment with febuxostat (80 mg) for 28 weeks, ~70% of patients showed blood UA ≤6.0 mg/L (Tayar et al., 2012). However, one population-based cohort study in Asians during 2012–2016 showed that febuxostat carried the risks of cardiovascular diseases and related deaths (Chen et al., 2019a). A multicenter, double-blind, noninferiority trial involving >6000 patients with gout and cardiovascular diseases reported the high all-cause mortality and cardiovascular mortality associated with febuxostat use (White et al., 2018). Therefore, XOR inhibitors need to be optimized further.

In recent years, our studies have concentrated on finding novel drugs for hyperuricemia treatment. WN1703 is a pyrazole derivative through the lead optimization of febuxostat *via* the bioisosterism strategy. Previously, we showed that WN1703 had a similar XOR-inhibitory effect to that of febuxostat *in vitro*. WN1703 could reduce the UA level significantly in mice suffering from acute or long-term hyperuricemia, and was similar to the effect of febuxostat. Besides, pathological results in mice with hyperuricemia showed that WN1703 and febuxostat could reduce kidney injury to some degree (Li et al., 2017b). Zhou and our colleagues carried out a preliminary pharmacokinetic study of WN1703 in rats. It showed that the time to maximum plasma concentration of WN1703 and its metabolites was <1 h, which was different to that of febuxostat. They predicted that WN1703 and its major metabolites had low hepatotoxicity according to the PROTOX-II data platform (Zhou et al., 2020). According to modified-Koch method, a toxicological study of WN1703 in rats showed that its median lethal dose was 1493.96 mg/kg. The main toxicity of WN1703 was presented as hepatotoxicity and nephrotoxicity at high doses (>1400 mg/kg). We consider that more systematic and in-depth pharmacodynamic research could be carried out on WN1703.

Yeast extract paste (YEP) could simulate the disorder of purine metabolism and increase the UA level caused by humans eating food with high purine content. In the present study, a model of metabolic disorders in rats was induced through YEP and potassium oxonate to evaluate the pharmacodynamic effect of WN1703. Results indicated that the levels of UA and blood urea nitrogen (BUN) in WN1703 groups were significantly lower than those in the model group and similar to those in the control group and febuxostat group. Besides, the antioxidation capacity of WN1703 groups was markedly higher than that of febuxostat. Overall, we showed that WN1703 had attractive pharmacodynamic activity in experimental rats, which merits further study.

2. Materials and methods

WN1703 was synthesized by our research team (purity ≥97% by high-performance liquid chromatography) (Li et al., 2017b). Potassium oxonate (purity >98%) was obtained from Shanghai yuanye Bio-Technology (Shanghai, China). Febuxostat (purity ≥97%) and sodium carboxymethyl cellulose (CMC-Na; United States Pharmacopeia grade) were purchased from Aladdin Biochemical Technology (Shanghai, China). Febuxostat and potassium oxonate were dissolved in 0.5% CMC-Na solution. WN1703 was diluted to 2.5, 5.0, and 10.0 mg/mL with 0.5% CMC-Na solution. YEP (purity >98%) was purchased from Beijing Aoboxing Bio-Technology (Beijing, China). Yeast feed was made by Nantong Trophy Feed Technology (Nantong, China). Yeast paste was mixed evenly into crushed standard feed at a 1:4 ratio, pressed into pellets, and sterilized by radiation. Standard feed was provided by the Laboratory Animal Center of South China University of Technology (Guangzhou, China). All assay kits used were obtained from NanJing JianCheng Bioengineering Institute (Nanjing, China). Antibodies against XOR, URAT1, and IgG(H&L) were purchased from Abcam (Cambridge, UK).

2.1. Animals

The study protocol was approved (20180009) by the Ethics Committee of South China University of Technology (Guangzhou, China).

Forty-eight specific pathogen-free male SD rats (160–200 g) were purchased from Hunan Sleke Jingda Experimental Animals (SYXK (Guangdong) 2017–0178; Guangzhou, China). The cage temperature was 20–26 °C and the relative humidity was 40–70%. Rats were given standard feed adaptively for 1 week. During consecutive administration for 35 days, food was withheld for 12 h per 7 days, but water was freely available.

2.2. Animal model of hyperuricemia and drug administration

Rats were divided randomly into six groups of eight: control (CG), model (MG), febuxostat (5.0 mg/kg; FEB) (Sánchez-Lozada et al., 2008), low dose of WN1703 (2.5 mg/kg; L1703), median dose of WN1703 (5.0 mg/kg; M1703), and high dose of WN1703 (10.0 mg/kg; H1703). Except for the CG, rats in the other five groups were fed YEP and given potassium oxonate (750 mg/kg bodyweight, p.o.) every day, whereas rats in the CG were given standard feed and 0.5% CMC-Na at the same volume by oral administration. Rats were anesthetized with ether to take 1 mL of blood from the inner canthus every 7 days. Blood samples were centrifuged (1640×*g*, 10 min, 4 °C), and the upper serum was stored at −80 °C for measurement.

At study termination, all rats were fasted for 12 h without water restriction. Then, rats in each group were anesthetized with 20% urethane (0.3 mL/100 g bodyweight, i.p.). When the eyelid reflex disappeared, blood was taken from the abdominal aorta, and centrifuged (1640×*g*, 10 min, 4 °C) after standing for 2 h at room temperature. Serum was separated and stored at −80 °C. After blood had been taken and rats killed, the heart, kidney, and part of liver were taken and placed in formalin cups. Then, 4% paraformaldehyde solution was added to each cup. The remainder of fresh liver was washed with physiologic (0.9%) saline, placed in the pathology specimen bag, and stored at −80 °C.

2.3. Analyses of biochemical indices in serum

2.3.1. Serum pretreatment

Serum samples were thawed completely in an ice–water bath, and vortex-mixed (410×*g*, 2 min, 4 °C). The protein flocculent was precipitated and isolated, and the clear upper layer was employed for testing.

2.3.2. Pretreatment of liver samples

Liver tissue was weighed accurately. Physiologic saline was added at a ratio of 1:9 (*w:v*). Then, the mixture was homogenized mechanically in an ice–water bath and vortex-mixed (930×*g*, 10 min, room temperature). The supernatant was removed.

2.3.3. Measurement of levels of UA, BUN, creatinine, glucose, and triglycerides (TG) and other biochemical indicators in blood

Levels of UA, BUN, creatinine, glucose, TG and blood lipid (including TG, LDL-C, HDL-C and cholesterol) were measured by an automatic biochemical analyzer (AU5811; Beckman Coulter, Fullerton, CA, USA). The instrument was calibrated and used according to manufacturer instructions.

2.3.4. Measurement of antioxidant and anti-inflammatory markers

The activities of XOR, adenosine deaminase (ADA), and glutathione peroxidase (GSH-PX), and the level of malondialdehyde, were measured with colorimetric test kits. Levels of the proinflammatory factors monocyte chemoattractant protein (MCP)-1, tumor necrosis factor (TNF)-α, and IL-1β were measured with enzyme-linked immunosorbent assay (ELISA) kits. All measurements were carried out according to manufacturer instructions.

2.4. Collection and production of specimens

2.4.1. Hematoxylin and eosin (H&E) staining of tissue

Fresh tissues of the liver, kidneys, and heart were fixed in 4% paraformaldehyde for 24 h. After dehydration using a graded series of alcohol solutions, tissues were embedded in paraffin and sectioned into pieces of thickness 4 μm for staining. Stained pieces by eosin dye solution were sealed from dehydration. Images were analyzed under a microscope (DM4000 B LED; Leica MicrosystemsCMS GmbH, Wetzlar, Germany).

2.4.2. Tissue immunohistochemistry

Tissue slices were dewaxed and hydrated. Then, antigens were removed by placing the tissue slices in a microwave oven for 23 min. Hydrogen peroxide (3%) was added to slices to block endogenous peroxidase. After addition of 3% bovine serum albumin, primary and secondary antibodies were added to slices. 3, 3′-diaminobenzidine was used as a chromogenic reagent and hematoxylin was used to re-dye slices. Finally, treated slices were dehydrated and sealed with neutral gum for analyses.

2.5. Statistical analyses

Data are the mean ± standard deviation. One-way ANOVA was used for comparison among all six groups. The Student's *t*-test was employed for unpaired analysis. Data were processed with SPSS 19.0 (IBM, Armonk, NY, USA). $P < 0.05$ was considered significant.

3. Results

3.1. Health status of rats

The bodyweight of the six groups of rats at different times are listed in Fig. 1. There was no significant difference in bodyweight of rats in the six groups at experiment initiation. An increasing trend of bodyweight was much lower for rats in the MG from day-14 ($P < 0.05$) and rats appeared depressed, which suggested that the hyperuricemia model had been induced. For the FEB group, rats showed a similar change in bodyweight to that of the MG, and low spirits were not improved. The bodyweight and mental state of rats were improved after WN1703 intake. For example, the trend in bodyweight gain in the L1703 group and H1703 group was similar to that in the CG. We do not know why the trend in bodyweight gain of the M1703 group was not consistent with that of the other two WN1703 groups, but it was more effective in regulating the bodyweight of hyperuricemia-suffering rats and improving their mental state than that in the FEB group at the same dose.

3.2. UA level

The serum UA level of rats in different groups is shown in Table 1 and Fig. 2. There was no significant change in the UA level in the six groups at experiment initiation ($P > 0.05$). From day-14 of the experiment, the UA level of the MG increased ($P < 0.01$). Until day-35, the UA level of the MG increased to 4-times higher than that of the CG. This finding indicated that a stable and continuous hyperuricemia model of rats had been established by taking potassium oxonate (p.o.) combined with a yeast-paste diet. For the drug-administration groups, the UA level of rats in each group showed different degrees of change. The UA level in the FEB group decreased to an extent that there was a significant difference between the FEB group and MG ($P < 0.01$) from day-14, indicating that febuxostat had significant UA-lowering activity throughout the experiment. The UA-lowering effect of WN1703 in the three dose groups was not obvious at day-14, but a clear decrease in the UA level ($P < 0.01$) was shown from day-21, suggesting that WN1703 might work more slowly than febuxostat. Comparison of the UA levels between the FEB group and M1703 group at the same dose was revealed at day-14 ($P < 0.05$) but, from day-21 to day-35, there was no significant difference in UA levels between the two groups ($P > 0.05$). Hence, the UA-lowering potency of

Table 1
Level of uric acid in six groups of rats at different times during YEP-potassium oxonate-induced hyperuricemia.

Group	Day-0	Day-7	Day-14	Day-21	Day-28	Day-35
CG	107.4 ± 13.7	125.3 ± 32.1	121.1 ± 26.9**	110.5 ± 19.8**	119.8 ± 8.4**	94.7 ± 13.8**
MG	110.5 ± 12.1	127.8 ± 23.2	186.5 ± 32.3	180.3 ± 45.2	193.4 ± 39.9	432.5 ± 40.7
FEB	110.5 ± 4.4	127.8 ± 22.6	142.8 ± 35.1**	103.0 ± 7.7 **	127.9 ± 30.7**	127.3 ± 22.6**
L1703	105.8 ± 10.6	169.1 ± 41.3	200.3 ± 39.2	127.0 ± 36.8 **	154.3 ± 22.5**	145 ± 38.93**
M1703	104.3 ± 10.7	114.6 ± 27.5	171.8 ± 21.2$^{\#}$	117.1 ± 15.7 $^{\#}$**	122.1 ± 22.4**	133.4 ± 39.5**
H1703	114.4 ± 14.9	126.3 ± 31.7	170.9 ± 36.1	108.3 ± 33.7 **	145.1 ± 44.9**	126.3 ± 35.7**

Values are in μmol/L. Data are mean ± SD. n = 8. Compared with the MG, *$P <$ 0.05, **$P < 0.01$; compared with the FEB group, $^{\#}P < 0.05$, $^{\#\#}P < 0.01$.

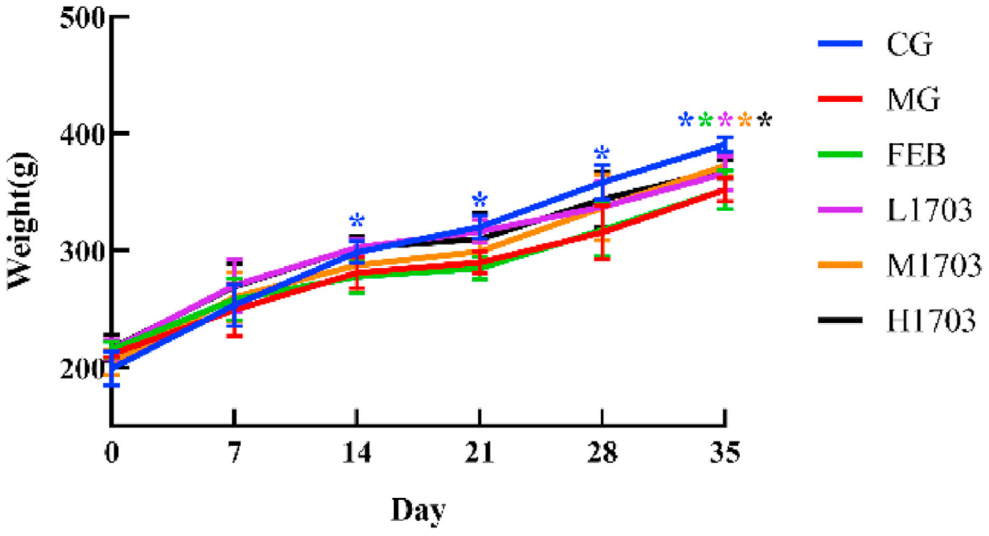

Fig. 1. Bodyweight of six groups of rats at different times during YEP-potassium oxonate-induced hyperuricemia. A: CG; B: FEB group; C: L1703 group; D: M1703 group; E: H1703 group. Compared with the MG, *$P < 0.05$.

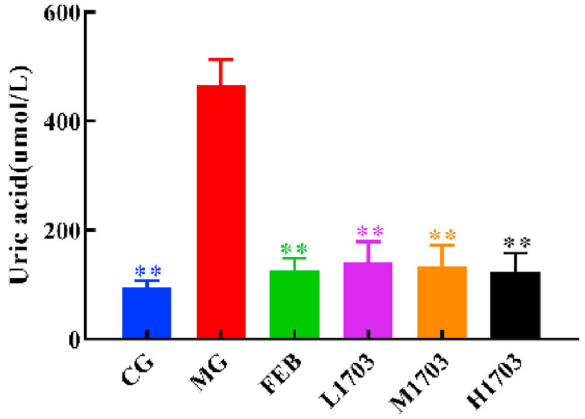

Fig. 2. Levels of uric acid in six groups of rats at experiment termination after YEP-potassium oxonate-induced hyperuricemia. Compared with the MG, $*P < 0.05$, $**P < 0.01$.

WN1703 was similar to that of febuxostat. Comparison of the UA level of the WN1703 groups at each detection point revealed the UA-lowering effect of WN1703 to improve in a dose-dependent manner.

3.3. *Levels of creatinine and BUN (Fig. 3)*

At experiment initiation (day-0), there was no significant difference in levels of creatinine or BUN ($P > 0.05$) among the six groups. With progress of the experiment, the levels of creatinine and BUN increased synchronously in each group. Compared with the CG, the BUN levels of MG rats showed an increasing trend ($P < 0.01$), and the creatinine levels of MG rats increased, but not significantly ($P > 0.05$). Compared with the MG group, the creatinine levels in the drug-administration groups showed a decreasing trend, but not significantly ($P > 0.05$). Among all administration groups, only the M1703 group and FEB group had a marked effect on the BUN level ($P < 0.05$), and the other groups had different influences on lowering the BUN level ($P > 0.05$).

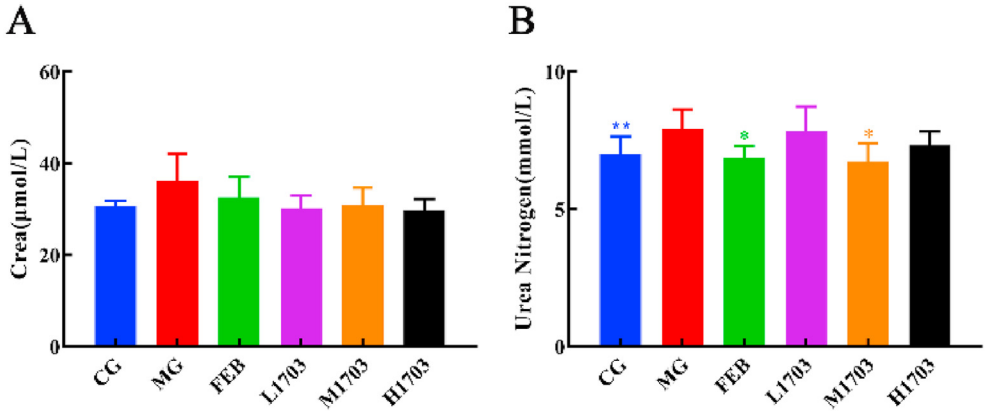

Fig. 3. Levels of creatinine and BUN in six groups rats at experiment termination after YEP-potassium oxonate-induced hyperuricemia. A: Creatinine; B: BUN. Compared with the MG, $*P < 0.05$, $**P < 0.01$.

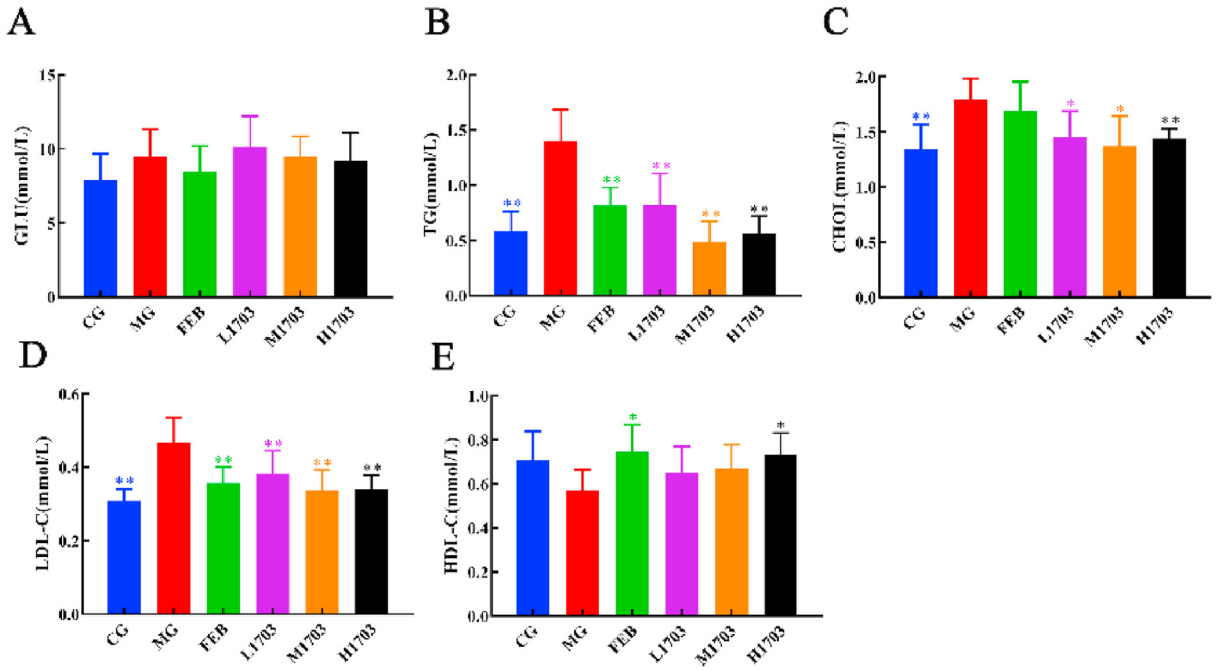

Fig. 4. Levels of glucose and lipids in six groups of rats at experiment termination after YEP-potassium oxonate-induced hyperuricemia. A: Glucose; B: TG; C: cholesterol; D: LDL-C; E: HDL-C. Compared with the MG, $*P < 0.05$, $**P < 0.01$.

3.4. Changes in blood levels of glucose, lipids, and other serum indices (Fig. 4)

Compared with the CG group, levels of TG, cholesterol, and low-density lipoprotein-cholesterol (LDL-C) of the MG showed a significantly rising trend ($P < 0.01$). Hence, MG rats were complicated with lipid and glucose-metabolism disorders, though levels of high-density lipoprotein-cholesterol (HDL-C) and glucose did not change significantly ($P > 0.05$). At an identical dose, WN1703 and febuxostat could reduce levels of TG ($P < 0.01$) and LDL-C ($P < 0.01$) in serum, but only febuxostat and a high dose of WN1703 could increase the HDL-C level of rats ($P < 0.05$). The three doses of WN1703 all had a more marked effect on lowering the cholesterol level than febuxostat. Hence, WN1703 was more effective in reducing levels of TG and cholesterol, but febuxostat had greater potential at increasing the HDL-C level, at the same dose.

3.5. Antioxidant capacity (Fig. 5)

The activity of superoxide dismutase (SOD) ($P < 0.05$) and GSH-PX ($P < 0.01$) in the serum of MG rats decreased, whereas the level of malondialdehyde increased significantly ($P < 0.01$), which suggested weakened antioxidant ability and enhanced lipid peroxidation was induced for MG rats. Febuxostat increased SOD activity significantly ($P < 0.01$), but a significant difference was not found for the regulatory effects of febuxostat on levels of GSH-PX or malondialdehyde (MDA) ($P > 0.05$). All groups of WN1703 could increase the SOD activity and reduce the MDA level in a dose-dependent manner. However, there was no difference in GSH-PX activity among the three WN1703 groups and MG ($P > 0.05$). At an identical dose, WN1703 and febuxostat could increase SOD activity, whereas WN1703 could also reduce the MDA level. Hence, WN1703 was much more potent in improving the antioxidant effect of hyperuricemia-suffering rats than febuxostat.

3.6. Activity of XOR and ADA (Fig. 6)

The activity of XOR and ADA in serum and liver homogenates was measured. Compared with the CG, the activity of XOR and ADA of MG rats was increased in serum ($P < 0.01$). Compared with the MG, the FEB group and three dose groups of WN1703 showed different degrees of inhibition of XOR and ADA activities. Febuxostat reduced the activity of XOR in serum ($P < 0.05$) and liver homogenates ($P < 0.05$), and inhibited ADA activity in serum ($P < 0.01$) and liver homogenates ($P < 0.01$) significantly. Hence, febuxostat was a good inhibitor of XOR and ADA. WN1703 also inhibited the activity of XOR and ADA in serum significantly in an approximately dose-dependent manner. At an identical dose, the inhibitory effect of WN1703 on the activity of XOR in serum and liver homogenates was stronger than that of febuxostat, but there was little difference between those two compounds in regulation of ADA activity in serum and liver homogenates.

3.7. Proinflammatory factors in serum (Fig. 7)

At experiment termination, the serum level of MCP-1 ($P < 0.01$), TNF-α ($P < 0.01$), and IL-1β ($P < 0.01$) in the MG group increased, which indicated an inflammatory process in the body with an increase in the UA level. Febuxostat showed a certain anti-inflammatory effect by the reducing the levels of MCP-1 ($P < 0.01$), TNF-α ($P < 0.01$), and IL-1β ($P < 0.05$). The three doses of WN1703 could decrease the level of MCP-1 ($P < 0.01$), but their effect on the release of TNF-α ($P > 0.05$) was not obvious, and only high dose of WN1703 could reduce the IL-1β level ($P < 0.05$). Therefore, the anti-inflammatory effect of febuxostat was more potent than that of WN1703 at an identical dose. The effect of febuxostat and WN1703 on release of proinflammatory cytokines was not completely consistent, which suggested that those two compounds might mediate the inflammatory response through different signaling pathways *in vivo*.

3.8. Pathological staining of kidney tissues

The ratio of rats with renal injury in the MG, FEB group, and L1703 group was 4/8, 2/8 and 3/8, respectively. Pathological staining of the kidneys of rats with the most severe lesions in each group were selected for display (Fig. 8). H&E staining of CG rats showed uniform staining of kidney tissue, normal morphology and structure of glomeruli, compact arrangement of renal tubular epithelial cells with uniform size, and no obvious inflammation. In the MG, pathological changes were observed in the renal-tissue cortices to varying degrees, with a small number of exfoliated tubular epithelial cells (black arrow), dilated tubules, and a protein-like structureless substance in the lumen (green arrow). Significant lesions were not observed in the glomerular structure, but distended renal tubules to varying degrees (yellow arrow) were observed in the FEB group, and the amount of protein-like structureless substances in the lumen was reduced significantly (green arrow). After administration of three doses of WN1703, all rats showed normal glomerular morphology and normal structure, and the epithelial cells of renal tubules were closely arranged and of identical size. Few protein-like structureless substances were observed in the L1703 group (green arrow), suggesting that WN1703 could improve the kidney damage caused by hyperuricemia in a dose-dependent manner.

3.9. Pathological staining of liver tissues

H&E staining of liver tissues (Fig. 9) in the CG showed a clear structure and orderly arrangement of hepatic cords, abundant cytoplasm of hepatocytes, normal morphology and structure, without obvious changes in hepatic sinuses or obvious inflammation. In the MG, there was marked degeneration and necrosis of hepatocytes, infiltration of many inflammatory cells (black arrow), a small amount of hepatocyte steatosis around the central vein, with round vacuoles of varying sizes in the cytoplasm (green circle). Hence, MG rats had dyslipidemia, which was consistent with the change in levels of TG, cholesterol, LDL-C, and HDL-C. After intervention with febuxostat or WN1703, the inflammatory response of rats in each treatment group was alleviated significantly and infiltration by inflammatory cells in FEB, L1703, and M1703 groups was reduced, whereas hepatocyte steatosis was obvious in those groups. With an increasing dose of WN1703, its protection of the liver improved and pathological changes were not observed in the liver of H1703 rats.

3.10. Pathological staining of heart tissues

The morphology and construction of heart tissue in rats in all groups was stained uniformly by H&E (Fig. 10). The morphology and structure of myocardial fibers were normal, regular and clear, and obvious inflammation or abnormalities in the interstitium were not observed. Hence, our hyperuricemia modelling and the drugs we used did not affect the heart of rats.

3.11. Liver immunohistochemistry (Fig. 11)

There was no obvious expression of XOR in the CG, but XOR expression in the MG was increased significantly ($P < 0.01$), and XOR was distributed mainly in hepatocyte interstices as brown-yellow lumps. Expression of XOR in the FEB group and three WN1703 groups was reduced significantly ($P < 0.01$), showing a punctate distribution. Semi-quantitative analysis by Image Plus showed that the average optical density of XOR in the MG group was significantly higher than that in the CG ($P < 0.01$, Fig. 13A). The average optical density of XOR in the FEB group and each dose of WN1703 groups decreased significantly ($P < 0.01$), but it seemed that WN1703 was more effective in reducing XOR expression than that of febuxostat at an identical dose. Therefore, we suggest that the UA-lowering effect of WN1703 was achieved by inhibiting the activity and interfering with expression of XOR in the liver.

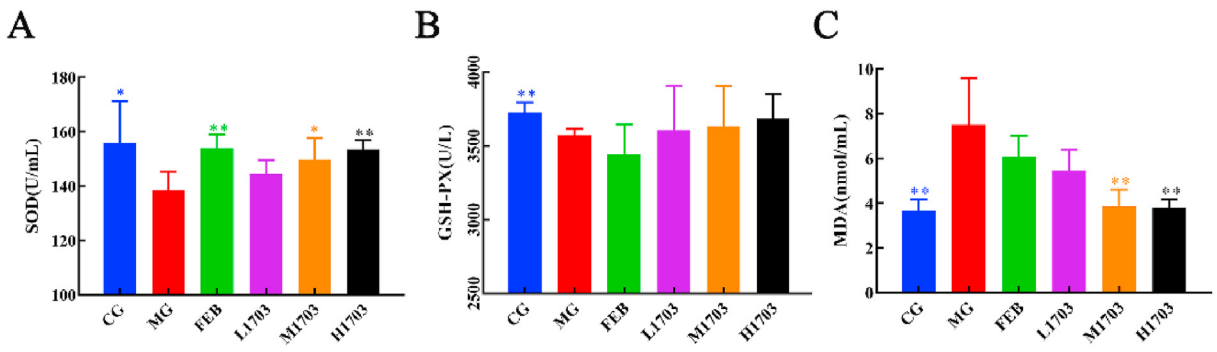

Fig. 5. Antioxidant capacity of WN1703 at experiment termination after YEP-potassium oxonate-induced hyperuricemia. A: SOD; B: GSH-PX; C: malondialdehyde (MDA). Compared with the MG, $^{*}P < 0.05$, $^{**}P < 0.01$.

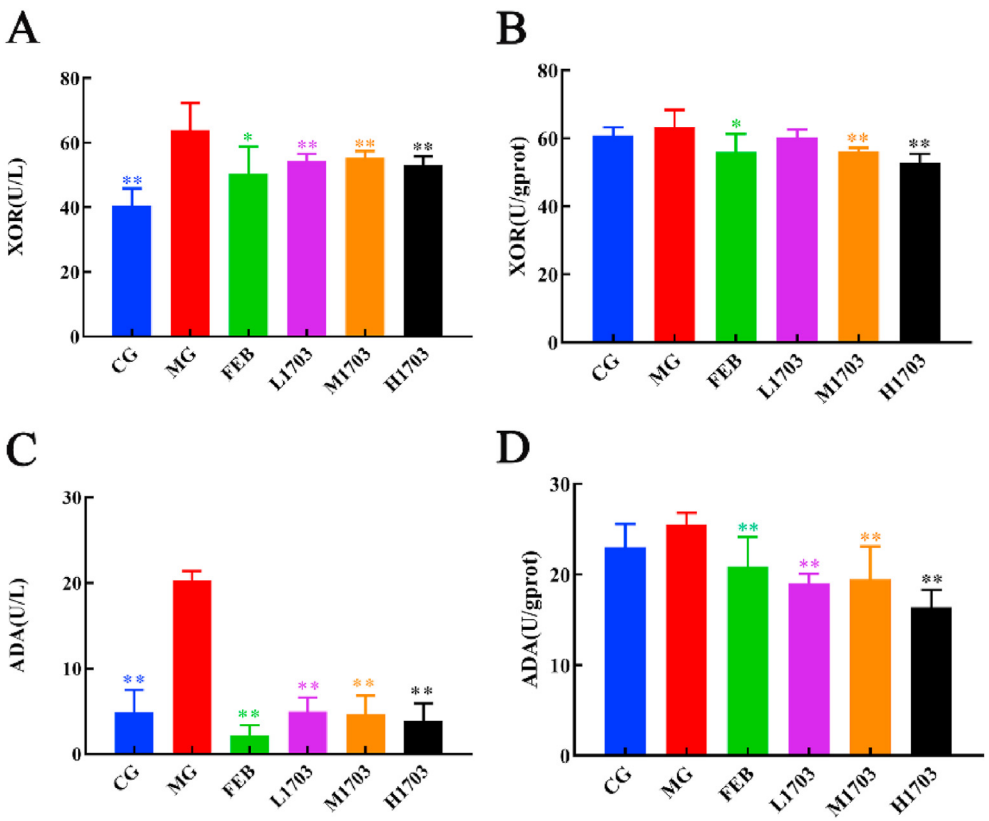

Fig. 6. Activity of XOR and ADA in six groups of rats at experiment termination after YEP-potassium oxonate-induced hyperuricemia. A: XOR activity in serum; B: XOR activity in liver homogenates; C: ADA activity in serum; D: ADA activity in liver homogenates. Compared with the MG, $^{*}P < 0.05$, $^{**}P < 0.01$.

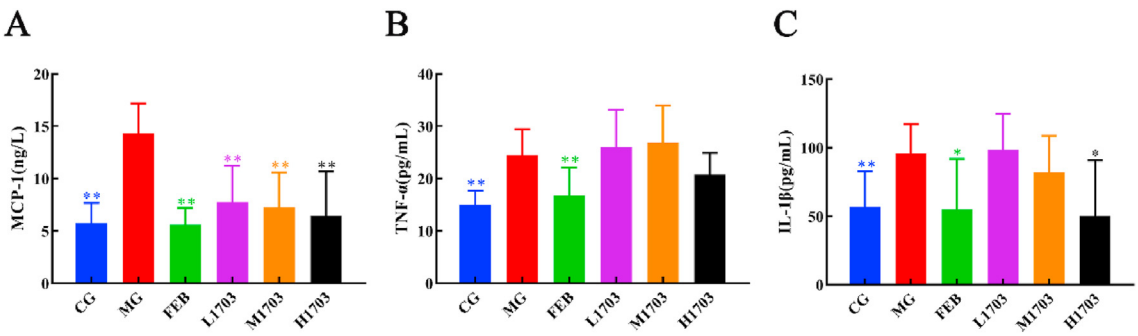

Fig. 7. Levels of MCP-1, TNF-α, and IL-1β in six groups of rats at experiment termination after YEP-potassium oxonate-induced hyperuricemia. A: MCP-1; B: TNF-α; C: IL-1β. Compared with the MG, $^{*}P < 0.05$, $^{**}P < 0.01$.

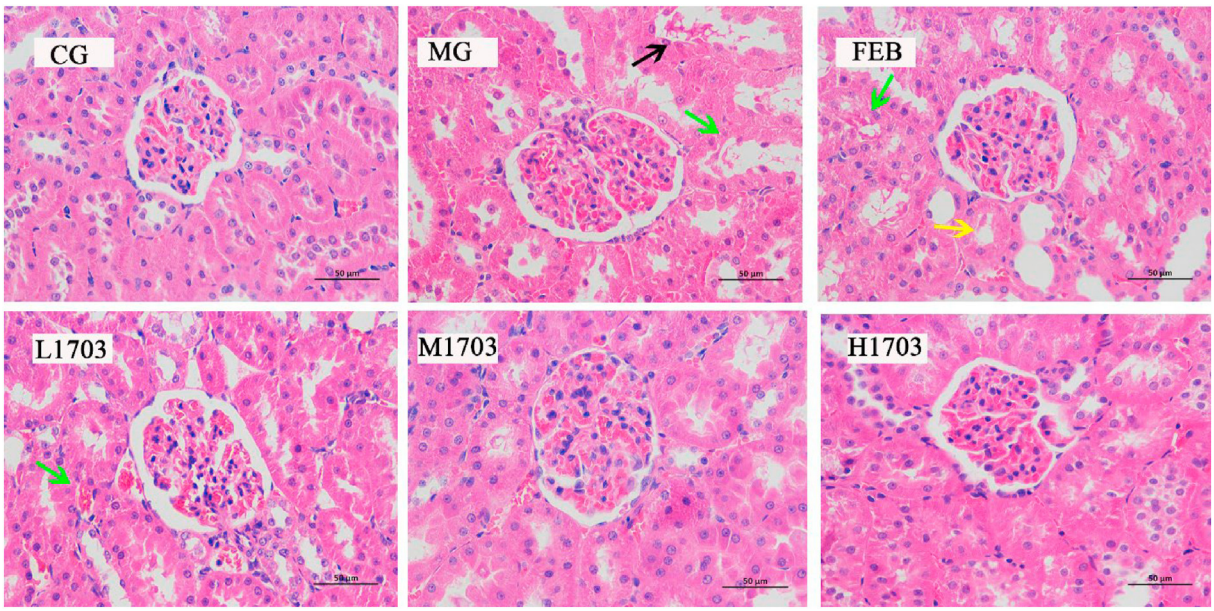

Fig. 8. Pathological changes in the renal tissue of six groups rats at experiment termination after YEP-potassium oxonate-induced hyperuricemia (H&E staining, × 400).

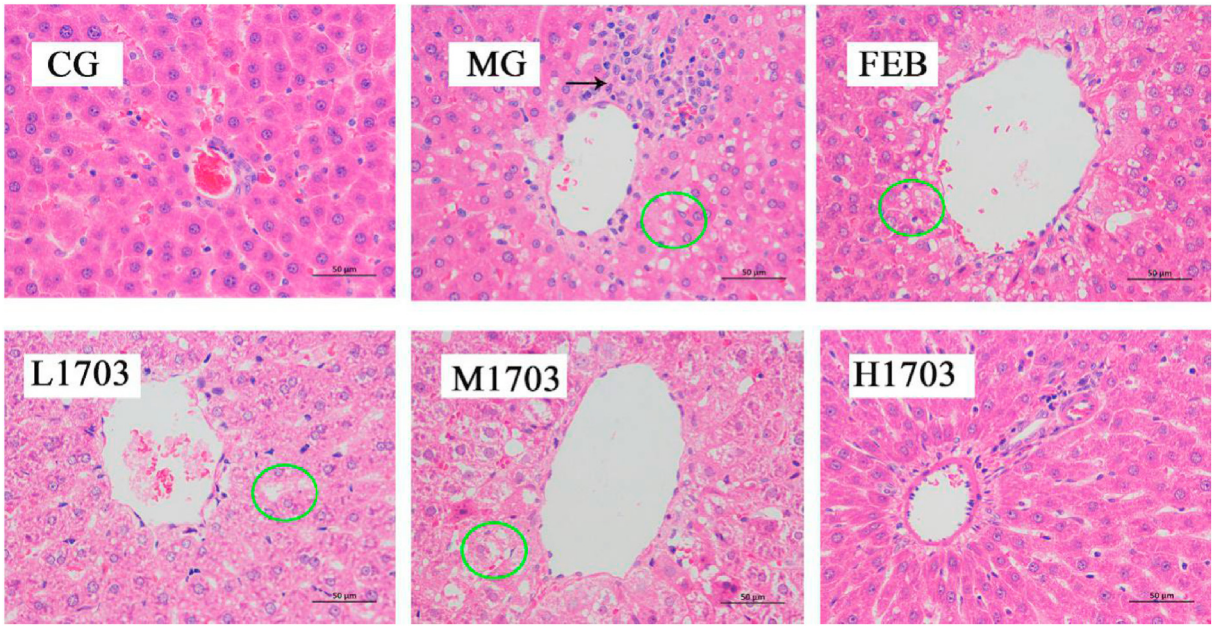

Fig. 9. Pathological changes in the liver tissue of six groups of rats at experiment termination after YEP-potassium oxonate-induced hyperuricemia (H&E staining, × 400).

3.12. Kidney immunohistochemistry

Weakly positive expression of URAT1 protein was found in the MG and each administration group except the CG (Fig. 12). The cytoplasm of renal cells was brown-yellow lumps dotted along the edge of renal tubules. Semi-quantitative analysis by Image Plus showed that the average optical density of URAT1 in the MG group was increased significantly ($P < 0.01$, Fig. 13B) compared with the CG. Administration of febuxostat and various doses of WN1703 did not affect URAT1 expression in the kidney ($P > 0.05$). Therefore, the UA-lowering effect of WN1703 and febuxostat was not relevant for regulating URAT1 expression in the kidney.

4. Discussion

Yeast extracts are rich in purine, which is regarded as a precursor of UA production. Yeast extracts can stimulate UA synthesis, and lead to purine-metabolism disorders. Increased UA levels can be induced by yeast-rich diets, oral administration of purine, or intraperitoneal injection of potassium oxonate or fructose (Wang et al., 2018; Xu et al., 2021; Lee et al., 2021; Hwa et al., 2011; Ghasemi, 2021; Lu et al., 2020; Álvarez-Lario and Alonso-Valdivielso, 2014; Zhang et al., 2020b; Shi et al., 2020; Chau et al., 2019). In the above studies, some researchers suggested that elevated blood glucose and lipids caused by hyperuricemia should be related to the injury of islet cell in high uric acid state. We

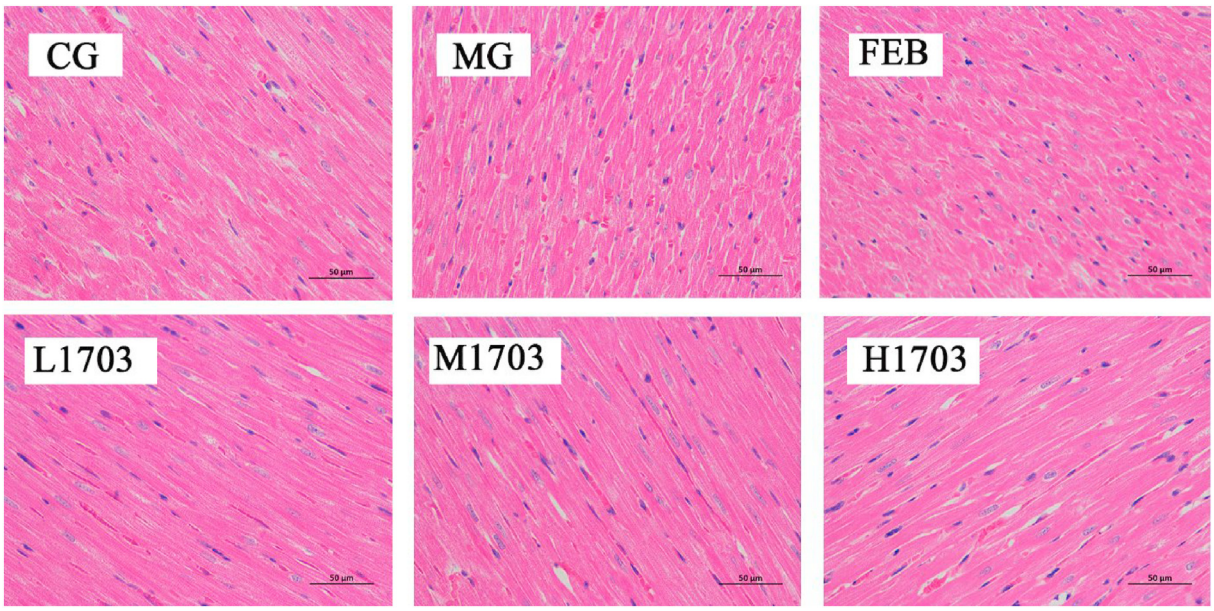

Fig. 10. Pathological changes in the heart tissue of six groups of rats at experiment termination after YEP-potassium oxonate-induced hyperuricemia (H&E staining, × 400).

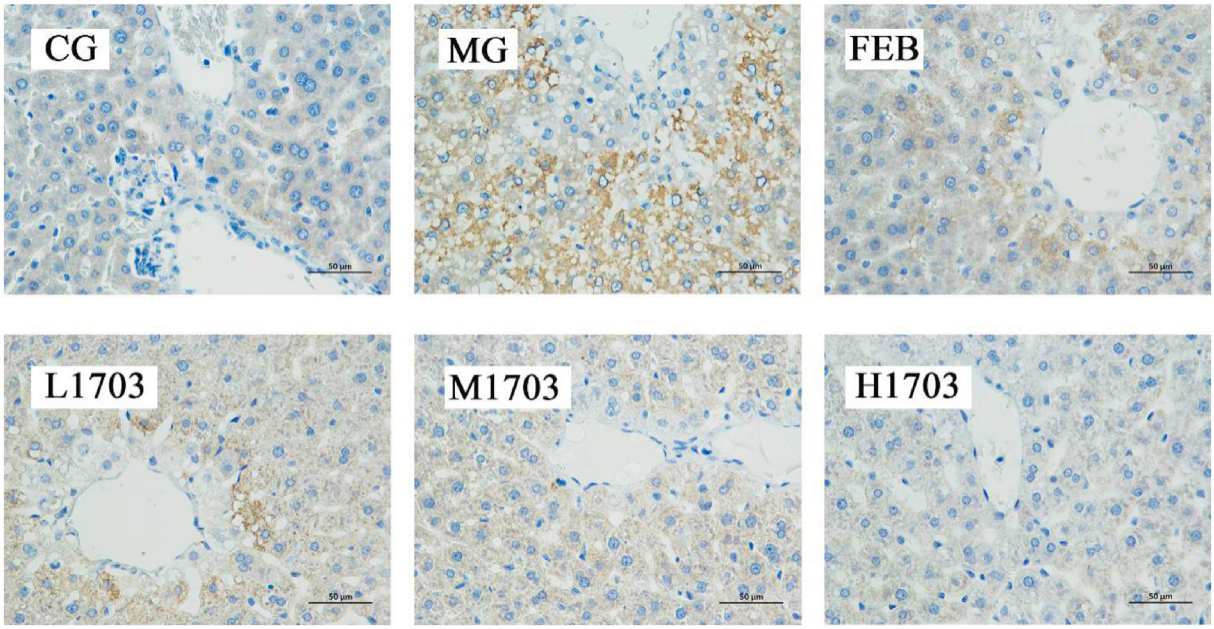

Fig. 11. Immunohistochemistry of XOR in the liver tissue of six groups of rats at experiment termination after YEP-potassium oxonate-induced hyperuricemia (× 400).

used the modelling method of potassium oxonate combined with YEP because of its simple operation. Furthermore, rats suffering from chronic hyperuricemia with a stable, high UA level could be obtained, accompanied by severe renal dysfunction and disorders of glucose and TG. Therefore, we obtained the animal model needed for our study readily and evaluated the pharmacodynamic effect of WN1703, without considering the regulating mechanism of WN1703 on blood glucose and lipids under existing conditions. In the follow-up studies, we will carry out relevant research *in vitro* and *in vivo*.

We demonstrated that WN1703 was an effective UA-lowering compound. It could simultaneously relieve renal injury, regulate lipid metabolism, and improve anti-inflammatory and antioxidant activity. It seemed that WN1703 was more effective than febuxostat in inhibiting XOR expression and antioxidant activity. In general, the pharmacologic action of WN1703 increased as its dose of administration increased, thereby showing a clear dose–effect relationship. As we have discussed previously, the docking study showed that WN1703 formed increased π-π interaction than that of febuxostat, which may be the reason for the more effective activity of WN1703 than febuxostat (Li et al., 2017b). However, the comparison of pharmacokinetic parameters between WN1703 and febuxostat is needed to get fully understand for the difference in activity between those two compounds.

The UA-lowering activity of WN1703 was closely associated with inhibiting XOR activity. With the intake of high-purine feed, the XOR activity in serum and liver homogenates was enhanced. XOR activity in blood and liver homogenates was inhibited to varying degrees by

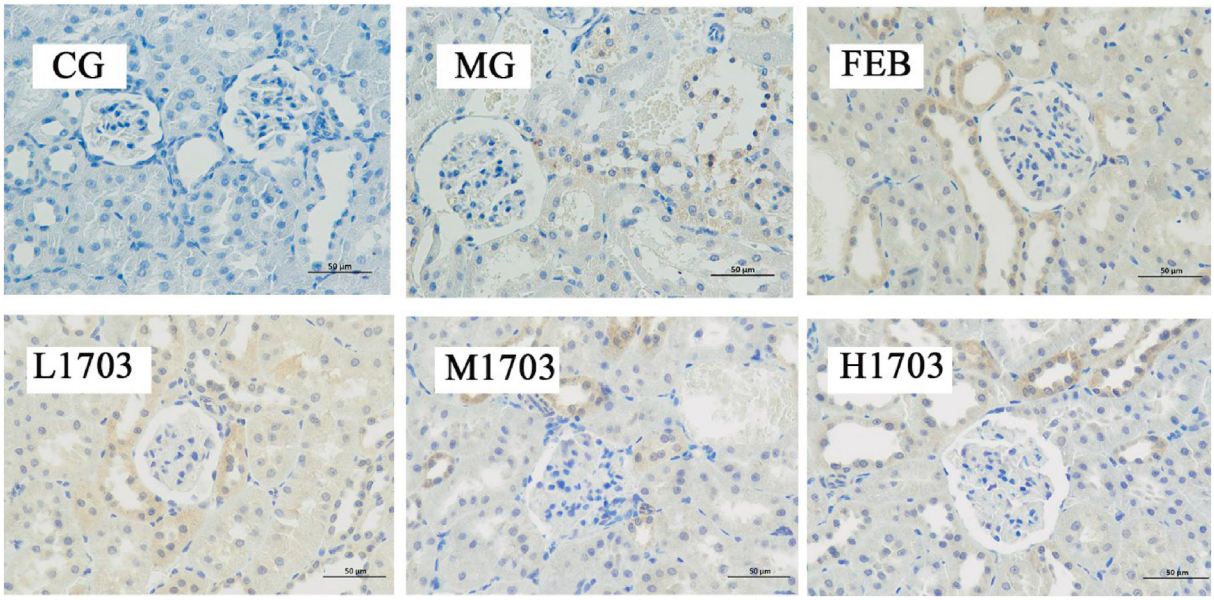

Fig. 12. Immunohistochemistry of URAT1 in the renal tissue of six groups of rats at experiment termination after YEP-potassium oxonate-induced hyperuricemia (× 400).

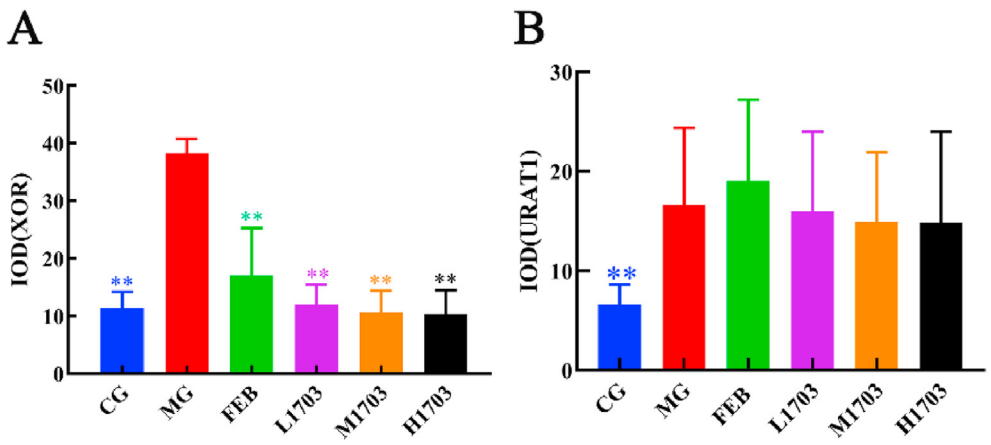

Fig. 13. Changes in expression of XOR and URAT1 in the liver and renal tissues, respectively, of six groups of rats at experiment termination after YEP-potassium oxonate-induced hyperuricemia. A: XOR; B: URAT1. Compared with the MG, $^{*}P < 0.05$, $^{**}P < 0.01$.

WN1703 administration. To our surprise, immunohistochemistry suggested that WN1703 administration could downregulate XOR expression in the liver. In summary, WN1703 could inhibit the catalytic activity of XOR, but also inhibit XOR expression. That is, WN1703 could reduce UA production through two mechanisms at least. How WN1703 inhibits XOR expression merits further research. We also focused on the effect of WN1703 on URAT1. Previously, we showed that WN1703 had only a slight inhibitory effect on URAT1 *in vitro* (Zhou et al., 2021). Here, we revealed the slight effect of WN1703 on URAT1 expression in the kidney. These results further suggested that the UA-lowering effect of WN1703 was mainly through interfering with XOR. In addition, WN1703 showed a significant effect in inhibiting ADA activity, thereby indicating that WN1703 may regulate multiple enzymes in the purine metabolic pathway.

If the concentration of UA exceeds its saturation concentration in body fluids, monosodium urate crystals are precipitated in tissues and induce inflammation, with increased release of proinflammatory cytokines such as TNF-α and IL-1β (Cabau et al., 2020). Besides, overloaded UA can cause a systemic response associated with oxidative stress, such as endothelial dysfunction and renal fibrosis (Glantzounis et al., 2005). In the present study, WN1703 alleviated the increasing trend of levels of TNF-α, IL-1β, MCP-1, and MDA in serum, and increased the activity of SOD and GSH-PX. Therefore, inflammation and peroxidation in rats were alleviated after WN1703 administration, indicating that WN1703 use could elicit comprehensive benefits besides its UA-lowering activity. At an identical dose, the ability of WN1703 to regulate GSH-PX activity and the MDA level was even higher than that of febuxostat.

The kidney is the main organ that excretes UA. A continuous increase in the UA level in the body will lead to glomerular-filtration dysfunction and then develop into renal injury (Lipkowitz, 2012; Garcia-Arroyo et al., 2018; Su et al., 2020). In general, levels of BUN and creatinine are used to evaluate renal function. However, because of strong renal compensation, these two parameters may show an upward trend only in the early stage of renal injury, and not show a significant difference in level from that in a normal group (Chen et al., 2019b; Cui et al., 2020). We not find a significant difference in the creatinine level between the MG and CG, indicating that the renal function of rats was in the compensatory stage in the experimental period. However, half of the renal tissue of MG rats showed obvious structural changes, indicating that renal injury occurred. Although only the BUN level in the febuxostat group and WN1703 groups

at the same dose showed a significant difference compared with that in the MG, renal histopathology showed that the prevalence of renal injury in the administration groups was lower than that in the MG. Hence, WN1703 might improve the renal injury caused by hyperuricemia. We need to identify more sensitive and reliable parameters that could be used to evaluate early renal injury in future studies.

An abnormal increase in the UA level *in vivo* will have an impact on glucose and lipid metabolism. For example, levels of TG and cholesterol in blood were increased, and pathological examination of liver tissue showed a change in liver structure or even necrosis, indicating that the increase in the UA level interfered with normal lipid metabolism. WN1703 administration helped to reduce levels of TG and LDL-C, increase HDL-C levels, and improve liver lesions in rats. Hence, WN1703 may improve dyslipidemia and liver damage by reducing the UA level.

5. Conclusions

By regulating mainly XOR activity and expression, the significant UA-lowering effect of WN1703 was demonstrated. WN1703 also improved lipid-metabolism disorders, anti-inflammatory effects, and antioxidant effects. Since febuxostat has been reported to carry cardiovascular risks in clinical trials (White et al., 2018), systematic toxicology and pharmacokinetics research should be carried out to clarify the toxicity and *in vivo* mechanism of action of WN1703.

CRediT authorship contribution statement

Yuanyuan Li: Investigation, Visualization, Methodology, Writing – original draft, Conceptualization. **Xinying Zhu:** Investigation, Writing – original draft, Conceptualization. **Fuyao Liu:** Writing – original draft, Data curation, Formal analysis. **Wen Peng:** Writing – review & editing. **Lei Zhang:** Visualization, Validation. **Jing Li:** Conceptualization, Supervision.

Declaration of competing interest

The authors declare that they have no known competing financial interests or personal relationships that could have appeared to influence the work reported in this paper.

Acknowledgments

This work was supported by the Key-Area Research and Development Program of Guangdong Province(2020B010188001), Science and Technology Project of Guangzhou(202102080325) and Open project supported by Hebei Province Key Laboratory of Traditional Chinese Medicine Research and Development (ZYKF202001).

Appendix A. Supplementary data

Supplementary data to this article can be found online at https://doi.org/10.1016/j.crphar.2022.100098.

References

Álvarez-Lario, B., Alonso-Valdivielso, J.L., 2014. Hyperuricemia and gout; the role of diet. Nutr. Hosp. 29, 760–770.
Cabau, G., Crisan, T.O., Kluck, V., Popp, R.A., Joosten, L.A.B., 2020. Urate-induced immune programming: consequences for gouty arthritis and hyperuricemia. Immunol. Rev. 294, 92–105.
Chau, Y.T., Chen, H.Y., Lin, P.H., Hsia, S.M., 2019. Preventive effects of fucoidan and fucoxanthin on hyperuricemic rats induced by potassium oxonate. Mar. Drugs 17, 343.
Chen, C.H., Chen, C.B., Chang, C.J., Lin Jr., Y., Wang, C.W., Chi, C.C., Lu, C.W., Chen, W.T., Pan, R.Y., Su, S.C., Hsu, L.A., Chang, Y.C., Yu, K.H., Wu, Y.J.J., Lin, K.M., Hung, S.I., Chen, S.M., Chung, W.H., 2019a. Hypersensitivity and cardiovascular risks related to allopurinol and febuxostat therapy in Asians: a population-based cohort study and meta-analysis. Clin. Pharmacol. Ther. 106, 391–401.
Chen, Y., Li, C., Duan, S., Yuan, X., Liang, J., Hou, S., 2019b. Curcumin attenuates potassium oxonate-induced hyperuricemia and kidney inflammation in mice. Biomed. Pharmacother. 118, 109195.
Cui, D., Liu, S., Tang, M., Lu, Y., Zhao, M., Mao, R., Wang, C., Yuan, Y., Li, L., Chen, Y., Cheng, J., Lu, Y., Liu, J., 2020. Phloretin ameliorates hyperuricemia-induced chronic renal dysfunction through inhibiting NLRP3 inflammasome and uric acid reabsorption. Phytomedicine 66, 153111.
Dehlin, M., Jacobsson, L., Roddy, E., 2020. Global epidemiology of gout: prevalence, incidence, treatment patterns and risk factors. Nat. Rev. Rheumatol. 16, 380–390.
Garcia-Arroyo, F.E., Gonzaga, G., Munoz-Jimenez, I., Blas-Marron, M.G., Silverio, O., Tapia, E., Soto, V., Ranganathan, N., Ranganathan, P., Vyas, U., Irvin, A., Ir, D., Robertson, C.E., Frank, D.N., Johnson, R.J., Sanchez-Lozada, L.G., 2018. Probiotic supplements prevented oxonic acid-induced hyperuricemia and renal damage. PLoS One 13, e0202901.
Ghasemi, A., 2021. Uric acid-induced pancreatic β-cell dysfunction. BMC Endocr. Disord. 21, 24.
Glantzounis, G.K., Tsimoyiannis, E.C., Kappas, A.M., Galaris, D.A., 2005. Uric acid and oxidative stress. Curr. Pharmaceut. Des. 11, 4145–4151.
Gliozzi, M., Malara, N., Muscoli, S., Mollace, V., 2016. The treatment of hyperuricemia. Int. J. Cardiol. 213, 23–27.
Hwa, K.S., Chung, D.M., Chung, Y.C., Chun, H.K., 2011. Hypouricemic effects of anthocyanin extracts of purple sweet potato on potassium oxonate-induced hyperuricemia in mice. Phytother Res. 25, 1415–1417.
Lee, D., Kim, J.K., Han, Y., Park, K.I., 2021. Antihyperuricemic effect of dendropanax morbifera leaf extract in rodent models. Evid Based Complement Alternat Med 2021, 3732317.
Li, Q., Li, X., Kwong, J.S., Chen, H., Sun, X., Tian, H., Li, S., 2017a. Diagnosis and treatment for hyperuricaemia and gout: a protocol for a systematic review of clinical practice guidelines and consensus statements. BMJ Open 7, e014928.
Li, J., Wu, F., Liu, X., Zou, Y., Chen, H., Li, Z., Zhang, L., 2017b. Synthesis and bioevaluation of 1-phenyl-pyrazole-4-carboxylic acid derivatives as potent xanthine oxidoreductase inhibitors. Eur. J. Med. Chem. 140, 20–30.
Lipkowitz, M.S., 2012. Regulation of uric acid excretion by the kidney. Curr. Rheumatol. Rep. 14, 179–188.
Lu, J., He, Y., Cui, L., Xing, X., Liu, Z., Li, X., Zhang, H., Li, H., Sun, W., Ji, A., Wang, Y., Yin, H., Li, C., 2020. Hyperuricemia predisposes to the onset of diabetes via promoting pancreatic β-cell death in uricase-deficient male mice. Diabetes 69, 1149–1163.
Miyake, T., Kumagi, T., Furukawa, S., Hirooka, M., Kawasaki, K., Koizumi, M., Todo, Y., Yamamoto, S., Abe, M., Kitai, K., Matsuura, B., Hiasa, Y., 2014. Hyperuricemia is a risk factor for the onset of impaired fasting glucose in men with a high plasma glucose level: a community-based study. PLoS One 9, e107882.
Sánchez-Lozada, L.G., Tapia, E., Soto, V., Avila-Casado, C., Franco, M., Zhao, L., Johnson, R.J., 2008. Treatment with the xanthine oxidase inhibitor febuxostat lowers uric acid and alleviates systemic and glomerular hypertension in experimental hyperuricaemia. Nephrol. Dial. Transplant. 23 (4), 1179–1185.
Shi, H., Liang, X.S., Huang, L.W., Luo, Z.G., Tan, L., 2020. The optimization and assessment of the method for inducing hyperuricemia in rats. Chin. J. Physiol. 36, 223–227.
Su, H.Y., Yang, C., Liang, D., Liu, H.F., 2020. Research advances in the mechanisms of hyperuricemia-induced renal injury. BioMed Res. Int. 2020, 5817348.
Tayar, J.H., Lopez-Olivo, M.A., Suarez-Almazor, M.E., 2012. Febuxostat for treating chronic gout. Cochrane 11, Cd008653.
Wang, K., Hu, L., Chen, J.K., 2018. RIP3-deficience attenuates potassium oxonate-induced hyperuricemia and kidney injury. Biomed. Pharmacother. 101, 617–626.
White, W.B., Saag, K.G., Becker, M.A., Borer, J.S., Gorelick, P.B., Whelton, A., Hunt, B., Castillo, M., Gunawardhana, L., 2018. Cardiovascular safety of febuxostat or allopurinol in patients with gout. N. Engl. J. Med. 378, 1200–1210.
Wu, A.H., Gladden, J.D., Ahmed, M., Ahmed, A., G, 2016. Filippatos, Relation of serum uric acid to cardiovascular disease. Int. J. Cardiol. 213, 4–7.
Xu, L., Lin, G., Yu, Q., Li, Q., Mai, L., Cheng, J., Xie, J., Liu, Y., Su, Z., Li, Y., 2021. Anti-hyperuricemic and nephroprotective effects of dihydroberberine in potassium oxonate- and hypoxanthine-induced hyperuricemic mice. Front. Pharmacol. 12, 645879.2.
Zhang, J., Zheng, R., Li, H., Guo, J., 2020a. Serum uric acid and incident atrial fibrillation: a systematic review and dose-response meta-analysis. Clin. Exp. Pharmacol. Physiol. 47, 1774–1782.
Zhang, C., Li, L., Zhang, Y., Zeng, C., 2020b. Recent advances in fructose intake and risk of hyperuricemia. Biomed. Pharmacother. 131, 110795.
Zhou, L., Wei, B., Wu, L., Li, J., Zhu, B., Zhang, L., 2020. Anti-hyperuricemia activity and toxicity prediction of a novel xanthine oxidoreductase inhibitor. Biomed. Chromatogr. : BMC (Biomed. Chromatogr.) 34, e4727.
Zhou, H., Zhong, G., Bai, J., Li, X., Peng, W., Zhang, L., Li, J., 2021. Development of a fluorescence-based assay for screening of urate transporter 1 inhibitors using 6-carboxyfluorescein. Anal. Biochem. 626, 114246.